

# Double percolation phase transition in clustered complex networks

Pol Colomer-de-Simón<sup>1</sup> and Marián Boguñá<sup>1</sup>

<sup>1</sup>*Departament de Física Fonamental, Universitat de Barcelona, Martí i Franquès 1, 08028 Barcelona, Spain*  
(Dated: September 11, 2022)

We perform an extensive numerical study of the effects of clustering on the structural properties of complex networks. We observe that strong clustering in heterogeneous networks induces the emergence of a core-periphery organization that has a critical effect on their percolation properties. In such situation, we observe a novel double phase transition, with an intermediate phase where only the core of the network is percolated, and a final phase where the periphery percolates regardless of the core. Interestingly, strong clustering makes simultaneously the core more robust and the periphery more fragile. These phenomena are also found in real complex networks.

PACS numbers:

The essence of complex systems lays on the interactions among their constituents. In many cases, these interactions are organized into complex topological architectures which have a determinant role on the behavior and functionality of this class of systems. Unlike regular lattices –where dimensionality seems to be the most distinctive feature– in complex networked systems, randomness and heterogeneity in their interactions induce phenomena that are very different from or even not observed in regular lattices. Examples range from the absence of epidemic thresholds separating healthy and endemic phases in scale-free networks [1–3] to anomalous behavior of Ising-like dynamics [4–7] and percolation properties [8–13].

Percolation theory has played a prominent role in the understanding of the anomalous behaviors we observe in complex networks. In fact, the percolation phenomenon is, in most cases, the common underlying principle behind them. Indeed, percolation is, for instance, strongly related to many types of epidemic-like processes on networks and it gives us important insights on the robustness of these networks to the failure of their constituents, a crucial issue for their functionality.

Interestingly, the interplay between a complex network topology and different percolation mechanisms leads to phenomena that are previously unseen in statistical physics. For instance, in standard site or bond percolation on top of random graphs with a power law degree distribution of the form  $P(k) \sim k^{-\gamma}$ , we observe a vanishing percolation threshold in the thermodynamic limit when  $\gamma \leq 3$  and anomalous critical exponents for  $3 < \gamma < 4$  [8, 10]. In non-equilibrium growing random networks, the percolation transition is of infinite order and the non-percolating phase is critical for any value of the occupation probability [14], with properties that are similar to the Berezinskii-Kosterlitz-Thouless phase transition [15, 16]. When two or more networks are interdependent, the failure of one node can potentially lead to a cascade process, leading to the disruption of a macroscopic portion of the whole system. This is similar to what happens in first order phase transitions, but with critical fluctuations in one of the sides of the critical point, suggesting that the transition is of hybrid na-

ture [17–19].

These phenomena are already observed on random graphs with given degree distributions. Random graphs of this kind are locally tree-like, that is, the number of triangles, and so the clustering coefficient, can be neglected in the thermodynamic limit. However, the high presence of triangles is, along with the small-world effect and the heterogeneity of the degree distribution, the most common and distinctive topological property of real complex networked systems. While we are certain that clustering is not a necessary condition for the emergence of any of these phenomena, we do not know how strong clustering can affect the percolation properties of the network. In this paper, we show that *strong clustering induces a core-periphery organization in the network giving rise to a new phenomenon, namely, a double percolation transition, where core and periphery percolate at different points.*

Here, we focus on the simplest percolation mechanism –bond percolation with bond occupation probability  $p$ – and study the effects that clustering has on the percolation threshold  $p_{th}$  and on the global topological structure of the network. Percolation on clustered networks has been studied in a number of research works. In general terms, they all agree that, above the threshold, clustering reduces the size of the giant component,  $G$ . However, they differ concerning on the position of the percolation threshold. Some studies report that clustered networks have a larger percolation threshold as compared to unclustered ones due to redundant edges in triangles that cannot be used to connect to the giant component [20–23]. Other studies report that strongly clustered networks are more resilient due to the existence of a core that is extremely difficult to break [24–26]. We shall show that, in fact, both arguments are correct, in the sense that clustering can make networks simultaneously more robust and less robust in front of the removal of their edges.

Throughout the paper, we use an ensemble of exponential random graphs with Hamiltonian

$$H = \sum_{k=k_{min}}^{k_c} |\bar{c}^*(k) - \bar{c}(k)|, \quad (1)$$

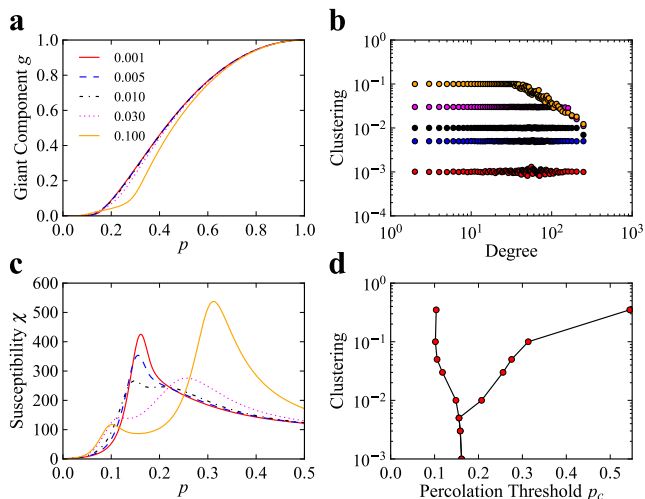


FIG. 1: Bond percolation simulations for networks with a power law degree distribution with  $\gamma = 3.1$  and different levels of clustering. (a) relative size of the largest connected component  $g$  as a function of the bond occupation probability  $p$ . (b) degree-dependent clustering coefficient  $\bar{c}(k)$ . (c) susceptibility  $\chi$  as a function of bond occupation probability  $p$ . (d) Percolation threshold ( $p_{max}$ ) as a function of the level of clustering.

where  $k_{min}$  and  $k_c$  are the minimum and maximum degrees of the network,  $\bar{c}(k)$  is the target degree-dependent clustering coefficient and  $\bar{c}^*(k)$  is the one corresponding to the current state of the network. We first generate a network with the configuration model (and thus unclustered) from a deterministic degree sequence drawn from a power law distribution with exponent  $\gamma$ . From this unclustered random network, the Hamiltonian in Eq. (1) is minimized by means of a simulated annealing procedure coupled to a Metropolis rewiring scheme until the current clustering is close enough to the target one. Rewiring events during the minimization of the Hamiltonian preserve both the degree distribution and the joint degree distribution of connected nodes,  $P(k, k')$ , so that degree-degree correlations are fully preserved [27] (see Appendix A) for further technical details). It is worth pointing out that networks generated in this way have global properties that are very similar to those observed in real networks [28].

A preliminary analysis shows that the percolation properties depend on two network features, the heterogeneity of its degree distribution and the shape of the clustering spectrum  $\bar{c}(k)$  [26]. For homogeneous networks, we observe that increasing the clustering in the network while keeping  $P(k, k')$  fixed increases the percolation threshold and decreases the size of the giant component (see Appendix B). However, the most interesting case corresponds to heterogeneous networks, typically with  $\gamma < 3.5$ . In this work, we focus on the case of  $\gamma = 3.1$  and a constant clustering spectrum [33]. This value of  $\gamma$  generates networks that are very heterogeneous

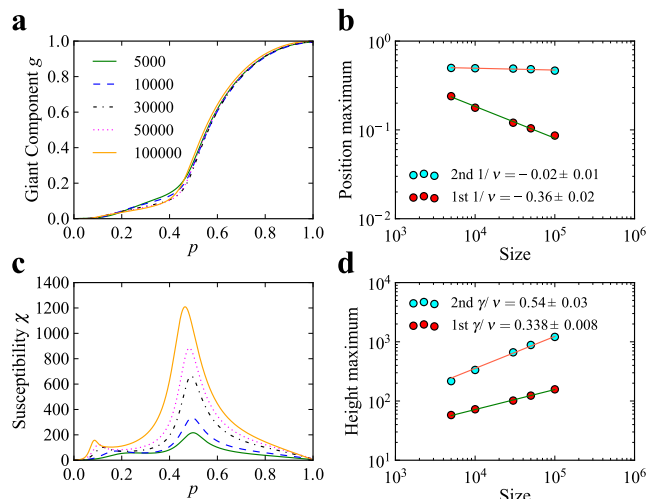


FIG. 2: Bond percolation simulations for networks with a power law degree distribution with  $\gamma = 3.1$ , target clustering spectrum  $\bar{c}(k) = 0.25$ , and different network sizes. (a) Size of the largest connected component  $S$  as a function of the bond occupation probability  $p$ . (c) Susceptibility  $\chi$  as a function of bond occupation probability  $p$ . (b) and (d) Position  $p_{max}$  and height  $\chi_{max}$  of the two peaks of  $\chi$  as function of network size  $N$ . The straight lines are power-law fits. (b) and (d) show the measured values of the critical exponents

without being scale-free, which allows us to clearly isolate the new phenomenon. Results for  $\gamma \leq 3$  are qualitatively similar –though more involved– and will be presented in a forthcoming publication.

Figure 1 shows the comparison of the percolation properties of networks with exactly the same degree sequence and degree-degree correlations but different levels of clustering. For each network, we perform bond percolation  $10^4$  times using the Newman–Ziff algorithm [29] and measure the average relative size of the largest (giant) connected component,  $g \equiv \langle G \rangle / N$ , and its fluctuations, *i.e.*, the susceptibility  $\chi = \sqrt{\langle G^2 \rangle - \langle G \rangle^2}$ . These results are then averaged over 200 network realizations. In finite systems, a peak in the susceptibility  $\chi$  indicates the presence of a continuous phase transition and its position gives an estimate of the percolation threshold. Plots (c) and (d) in Fig. 1 show new and surprising results. While for low levels of clustering there is a unique and well defined peak in  $\chi$ , increasing clustering gives rise to the emergence of a secondary peak at higher values of  $p$ . This fact suggests that we could be observing a double phase transition, where two different parts of the network percolate at different times.

To check this possibility, we perform finite size scaling on networks with target clustering spectrum  $c(k) = 0.25$  and different system sizes, ranging from  $N = 5 \times 10^3$  to  $N = 5 \times 10^5$ . Plot (d) in Fig. 2 shows that the susceptibility displays two peaks whose maxima  $\chi_{max}$  diverge as power laws,  $\chi_{max}(N) \sim N^{\gamma/\nu}$ . The position of the first peak approaches zero also as a power law

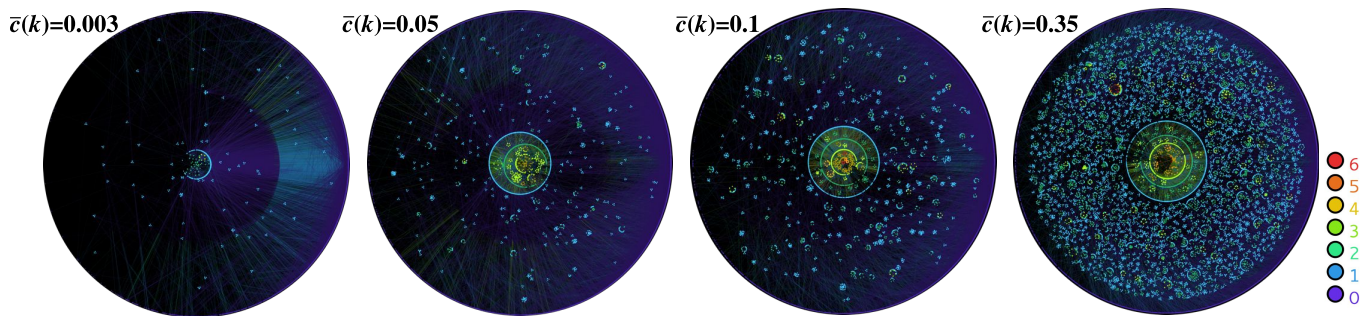


FIG. 3:  $m$ -core decomposition of four different networks with  $N = 5 \times 10^4$ ,  $\gamma = 3.1$ , and different levels of clustering,  $\bar{c}(k) = 0.003, 0.05, 0.1, 0.35$ . The color code of nodes represents the  $m$ -coreness of each node. For instance, nodes colored in violet belong to the  $m_0$ -core but not to the  $m_1$ -core and are said to have  $m$ -coreness zero. Nodes colored in blue belong to the  $m_1$ -core but not to the  $m_2$ -core and have  $m$ -coreness 1, etc. The visual representation is as follows. The outermost circle represents the  $m_0$ -core, with nodes of  $m$ -coreness 0 located in its perimeter and the  $m_1$ -core within the circle. When the  $m_1$ -core—which is contained within the  $m_0$ -core—is fragmented into different disconnected components, these are represented as non-overlapping circles within the outermost one and with nodes of  $m$ -coreness 1 located in their perimeters. The same process is repeated for each disconnected  $m_1$ -core, which will contain a subset of the  $m_2$ -core.

$p_{max}(N) \sim N^{1/\nu}$ , Fig. 2 (b), suggesting that even if the network is not scale-free, it is always percolated in the thermodynamic limit. The position of the second peak, instead, decreases very slowly, with an exponent that is compatible with zero. These facts confirm that, indeed, we are observing two different phase transitions. A first one between non-percolated/percolated phases and a second transition between two percolated phases with very different internal organization.

To understand the effect of clustering on the global structure of networks, it is useful to use the  $m$ -core decomposition developed in [28]. It is based on the idea of edge multiplicity  $m$ , defined as the number of triangles going through an edge. We further define the  $m$ -core as the maximal subgraph such that all its edges have, at least, multiplicity  $m$  within it. This defines a set of nested subgraphs that we call the  $m$ -core decomposition. This decomposition can be represented as a branching process encoding the fragmentation of  $m$ -cores into disconnected components as  $m$  is increased. The tree-like structure of this process informs us about the global organization of clustering in networks. To visualize this process we use the LaNet-vi 3.0 tool developed in [28]. Figure 3 shows the  $m$ -core decomposition of four networks with  $N = 5 \times 10^4$  nodes, the same degree sequence (with  $\gamma = 3.1$ ) and degree-degree correlations, and different levels of clusterings. As we can observe, for low levels of clustering the  $m_1$ -core is very small and so the  $m$ -core structure is almost inexistent. As clustering increases  $m$ -cores start developing new layers. For very high levels of clustering, the  $m_1$ -core is composed of a large connected cluster with a well developed internal structure—a core—and a large number of small disconnected components—a periphery—. This means that, even if the network is connected, by removing iteratively all edges with multiplicity zero, we end up with a small but well connected subgraph whereas the rest of the network is fragmented.

This suggests that the two peaks in the susceptibil-

ity could be related to this core-periphery organization. Both parts would percolate at different times, first the core and then the periphery, hence having their own percolation thresholds. To test this hypothesis, we perform bond percolation on the network with a bond occupation probability  $p$  laying between the two peaks. The giant component at this value of  $p$  defines a subgraph that we identify with the core and that roughly corresponds to the core observed in Figure 3, see Appendix C. Then, we extract from the original network the latter core subgraph, and what remains is then identified with the periphery. Once core and periphery are isolated, we perform bond percolation on them both independently and compare the results with the original network. Figure 4 shows that the core percolates at the point where the first peak appears in the original network, whereas the periphery percolates at the second peak.

Combining all these results, we can draw a general picture of the new phenomenon. High clustering in the network induces the emergence of a strongly entangled core and a weakly connected periphery. When bond occupation probability is increased from  $p = 0$ , there is a first phase transition where the core percolates. Rising  $p$  further, slowly increases the size of the core while the periphery still remains disconnected. Increasing  $p$  even further, we find a second phase transition where the periphery percolates. However, unlike ordinary percolation, this percolation event is independent of the fact that there is already a giant connected component in the network because, as shown in Fig. 4, the periphery does not need the core to percolate. We are thus in front of a phase transition between two different percolated phases. It is also interesting to notice that clustering affects the core and the periphery in opposite ways. Figure 1 (d) shows that when clustering is increased, the first peak moves to lower values of  $p$  whereas the second peak moves to higher values. This implies that while the core becomes

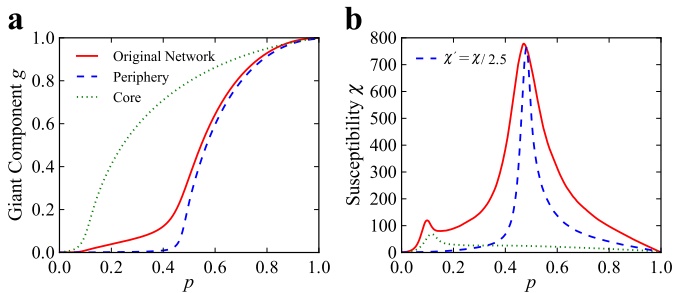


FIG. 4: Bond percolation simulations of the core and periphery of a network with  $N = 5 \times 10^4$ ,  $\gamma = 3.1$ , and target clustering spectrum  $\bar{c}(k) = 0.25$ . The bond occupation probability to separate the core is  $p = 0.2$ . The susceptibility curve of the periphery (dashed blue line) has been divided by 2.5 to ease the comparison.

more robust the periphery becomes more fragile.

This new phenomenon is also present in networks with different heterogeneities, including scale free networks. However, the behavior of the peaks is different depending on the heterogeneity. For homogeneous networks the core is not big enough to produce a measurable phase transition. Hence, only the phase transition of the periphery can be observed, which has a finite percolation threshold. For scale free networks, the percolation threshold of both peaks goes to zero in the thermodynamic limit, making the identification of the core more involved; it will be reported in a forthcoming publication. We finally note that this phenomenon is also present in many real complex networks. Figure 5 shows bond percolation experiments on top of the US air transportation network. In this case, we also observe a double peak in the susceptibility, suggesting that the network has a core-periphery organization. Results for other real networks are reported in Appendix D.

As we have seen, clustering has a non-trivial effect on the properties of complex networks. When clustering is strong enough, it induces the emergence of a core-periphery organization that redefines the percolation phase space of complex networks. Hence, there is a new percolated phase where the core of the network is percolated whereas the periphery is not. This new phase diagram implies the existence of a triple point yet to be characterized. Interestingly, increasing clustering makes the core of the network more robust whereas the periphery becomes more fragile. This reconciles the two dominant interpretations about the effect of clustering on the percolation properties of networks, which are then both correct. Our work opens new lines of research concerning the effect of this core-periphery architecture on dynamical processes taking place on networks. In the case of epidemic spreading, for instance, the core could act as a reservoir of infectious agents that would be latently active in the core while the rest of the network is uninfected.

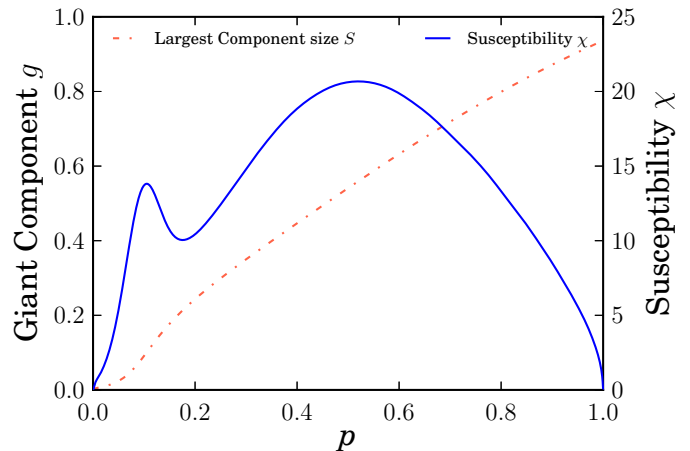


FIG. 5: Bond percolation simulations for the US air transportation network. (a) Relative size of the giant component  $g$  as a function of the bond occupation probability  $p$ . (b) susceptibility as a function of bond occupation probability  $p$ .

## Acknowledgments

This work was supported by a James S. McDonnell Foundation Scholar Award in Complex Systems; by the ICREA Academia prize, funded by the *Generalitat de Catalunya*; by MICINN project No. FIS2010-21781-C02-02; by *Generalitat de Catalunya* grant No. 2009SGR838; and by EC FET-Proactive Project MULTIPLEX (grant 317532).

## Appendix A: Maximally random clustered networks

Maximally random clustered networks are generated by means of a biased rewiring procedure. One edge is chosen at random that connects nodes A with B. Then, we choose at random a second link attached at least to one node (C) with the same degree of A. This link connects C with D. Then, the two edges are swapped so that nodes A and D, on the one hand, and C and B, on the other, are now connected. We take care that no self-connections or multiple connection between the same pair of nodes are created this process. Notice that this procedure preserves both the degree of each node and the actual nodes' degrees at the end of the two original edges. Therefore, the procedure preserves the full degree-degree correlation structure encoded in the joint distribution  $P(k, k')$ . The procedure is ergodic and satisfies detailed balance.

Regardless of the rewiring scheme at use, the process is biased so that generated graphs belong to an exponential ensemble of graphs  $\mathcal{G} = \{G\}$ , where each graph has a sampling probability  $P(G) \propto e^{-\beta H(G)}$ , where  $\beta$  is the inverse of the temperature and  $H(G)$  is a Hamiltonian that depends on the current network configuration. Here we consider ensembles where the Hamiltonian depends

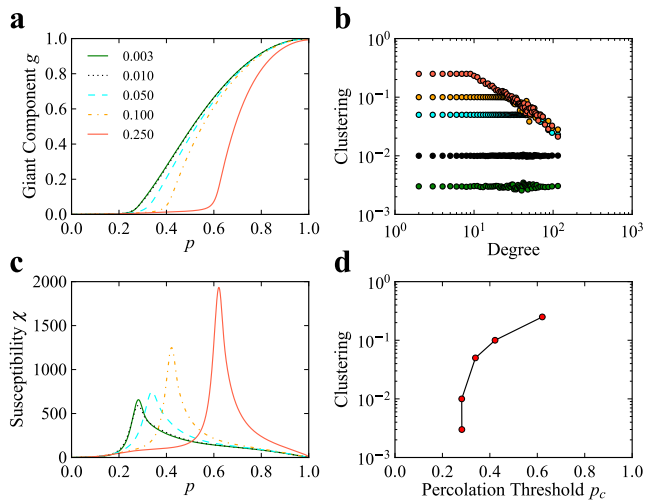


FIG. 6: Bond percolation simulations for networks with a power law degree distribution with  $\gamma = 3.5$  and different levels of clustering. (a) relative size of the largest connected component  $g$  as a function of the bond occupation probability  $p$ . (b) degree-dependent clustering coefficient  $\bar{c}(k)$ . (c) susceptibility  $\chi$  as a function of bond occupation probability  $p$ . (d) Percolation threshold ( $p_{max}$ ) as a function of the level of clustering.

on the target clustering spectrum  $\bar{c}(k)$  as

$$H = \sum_{k=k_{min}}^{k_c} |\bar{c}^*(k) - \bar{c}(k)|, \quad (A1)$$

where  $\bar{c}^*(k)$  is the current degree-dependent clustering coefficient. We then use a simulated annealing algorithm based on a standard Metropolis-Hastings procedure. Let  $G'$  be the new graph obtained after one rewiring event, as defined above. The candidate network  $G'$  is accepted with probability

$$p = \min(1, e^{\beta[H(G) - H(G')]} = \min(1, e^{-\beta\Delta H}), \quad (A2)$$

otherwise, we keep the graph  $G$  unchanged. We first start by rewiring the network  $200E$  times at  $\beta = 0$ , where  $E$  is the total number of edges of the network. Then, we start an annealing procedure at  $\beta_0 = 50$ , increasing the parameter  $\beta$  by a 10% after  $100E$  rewiring events have taken place. We keep increasing  $\beta$  until the target clustering spectrum is reached within a predefined precision or no further improvement can be achieved.

### Appendix B: Effect of clustering on homogeneous networks

Figures 6 for  $\gamma = 3.5$  and 7 for  $\gamma = 4$  show the comparison of the percolation properties of networks with exactly the same degree sequence and degree-degree correlations but different levels of clustering. For each network, we perform bond percolation  $10^4$  times using the

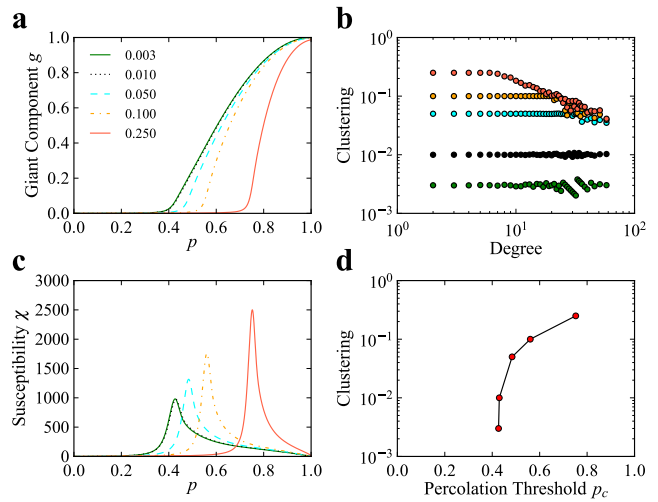


FIG. 7: Bond percolation simulations for networks with a power law degree distribution with  $\gamma = 4$  and different levels of clustering. (a) relative size of the largest connected component  $g$  as a function of the bond occupation probability  $p$ . (b) degree-dependent clustering coefficient  $\bar{c}(k)$ . (c) susceptibility  $\chi$  as a function of bond occupation probability  $p$ . (d) Percolation threshold ( $p_{max}$ ) as a function of the level of clustering.

Newman-Ziff algorithm [29] and measure the average relative size of the largest (giant) connected component,  $g \equiv \langle G \rangle / N$ , and its fluctuations, *i.e.*, the susceptibility  $\chi = \sqrt{\langle G^2 \rangle - \langle G \rangle^2}$ . These results are then averaged over 50 network realizations. In finite systems, a peak in the susceptibility  $\chi$  indicates the presence of a continuous phase transition and its position gives an estimate of the percolation threshold. All networks have a unique and well defined peak in  $\chi$ , and an increase of the clustering moves the peak to higher values of  $p$ . Hence clustering decreases the Giant component and increases the percolation threshold.

### Appendix C: Identification of the core

In order to identify which nodes belong to the core we perform bond percolation simulations with a bond occupation probability  $p$  that lays between the two percolation thresholds, *e.g.*  $p = 0.2$  for  $c(k) = 0.25$ . The giant component (GC) at this value  $p$  defines a subgraph that we identify with the core. Each bond percolation realization gives us a different GC, however, some nodes will belong more often to the GC than others. Hence, if one repeats this procedure many times, one can define the probability of a node to belong to the core, equal to, the fraction of times that a node belonged to the GC over the total number of bond percolation simulations. Figure 8 shows a network of 50.000 nodes, with a power law degree distribution with  $\gamma = 3.1$  and a clustering spectrum  $\bar{c}(k) = 0.25$ . The nodes are distributed according to its

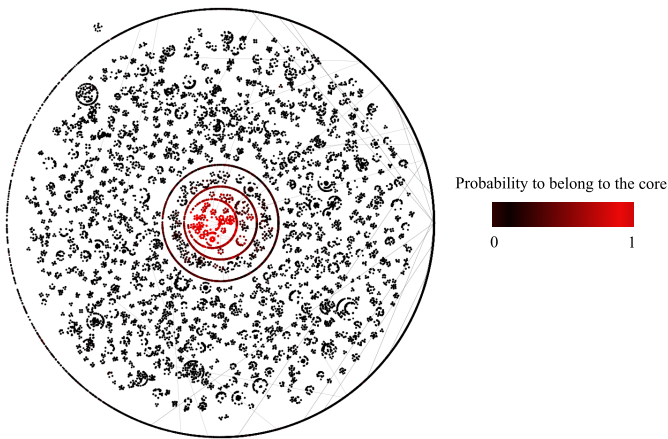


FIG. 8: A network of 50.000 nodes, with a power law degree distribution with  $\gamma = 3.1$  and a clustering spectrum  $\bar{c}(k) = 0.25$ . The nodes are distributed according to its  $m$ -core decomposition and their color goes from black (0) to red (1) proportional to the probability to belong to the giant component once we have performed bond percolation with  $p = 0.2$ .

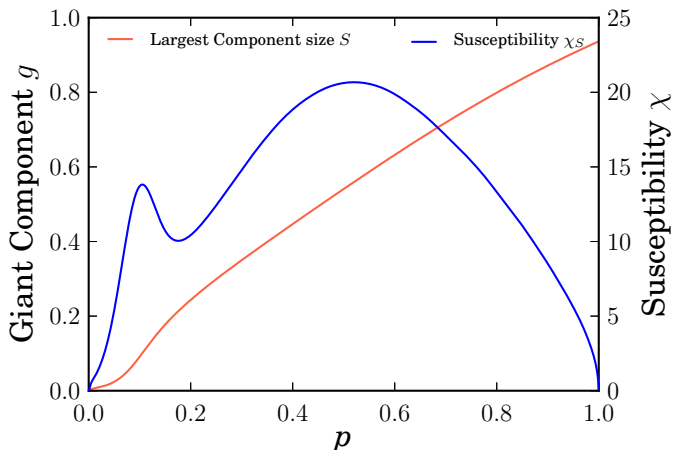


FIG. 9: Bond percolation simulations for the US air transportation network. Left Size of the largest connected component  $S$  as a function of the bond occupation probability  $p$ . Right susceptibility  $\chi_S$  as a function of bond occupation probability  $p$ .

$m$ -core decomposition but their color go from black (0) to red (1) proportional to the probability to belong to the core as defined before. The more red a node, the more probable that it belongs to the core. Here we can observe that, as we suggested, the core that we subtract in the paper is made mostly of nodes in the Giant component of the  $m_1$ -core of the network.

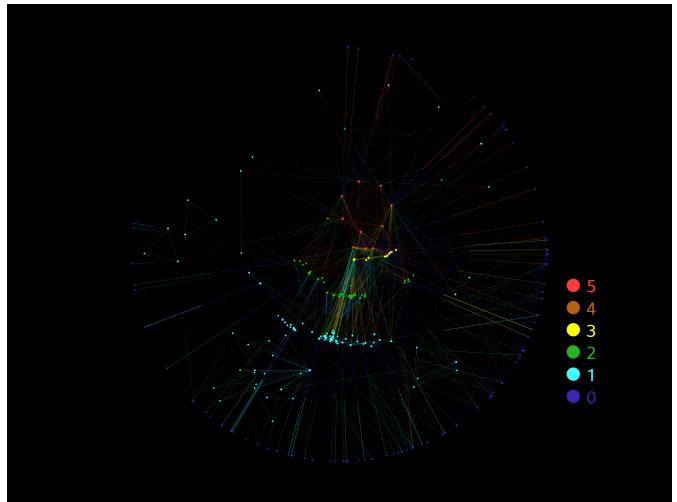


FIG. 10:  $m$ -core decomposition of the US air transportation network.

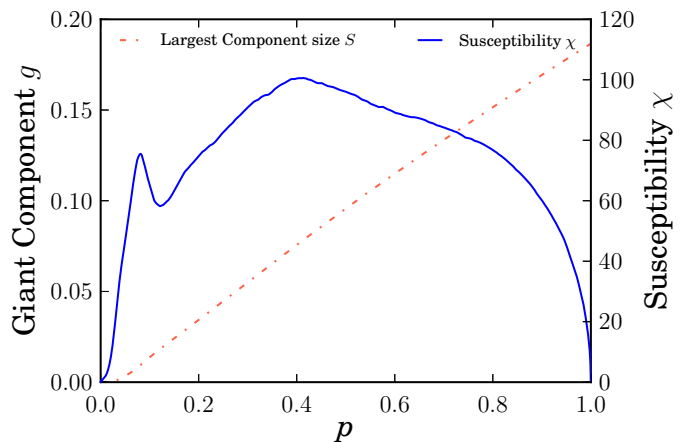


FIG. 11: Bond percolation simulations for the PGP network. Left Size of the largest connected component  $S$  as a function of the bond occupation probability  $p$ . Right susceptibility  $\chi_S$  as a function of bond occupation probability  $p$ .

## Appendix D: Real Networks

### 1. US air transportation network

In the US air transportation network the nodes are airports and a link is the existence of a direct flight between two airports. The data comes from ... The resulting network has 583 nodes, 1087 edges, an average degree of  $\bar{k} = 3.73$ , a clustering coefficient of  $\bar{C} = 0.43$  and a maximum degree of  $k_{max} = 109$ .

### 2. Pretty-Good-Privacy (PGP)

Pretty-Good-Privacy (PGP) is the most popular encryptor algorithm aimed to maintain privacy in communication between peers in internet. This algorithm makes

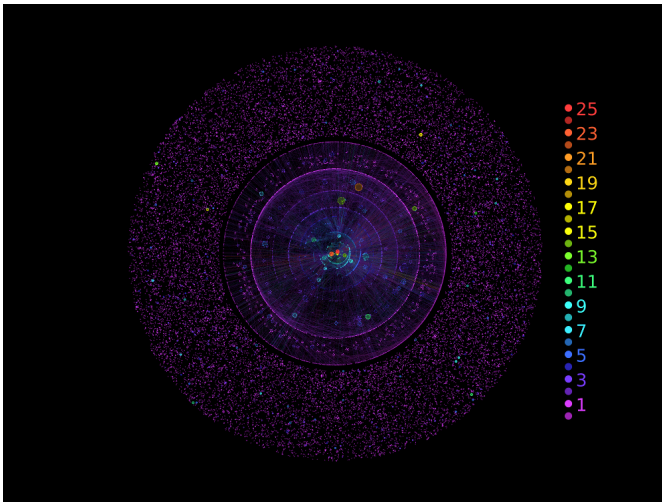


FIG. 12:  $m$ -core decomposition of the PGP network.

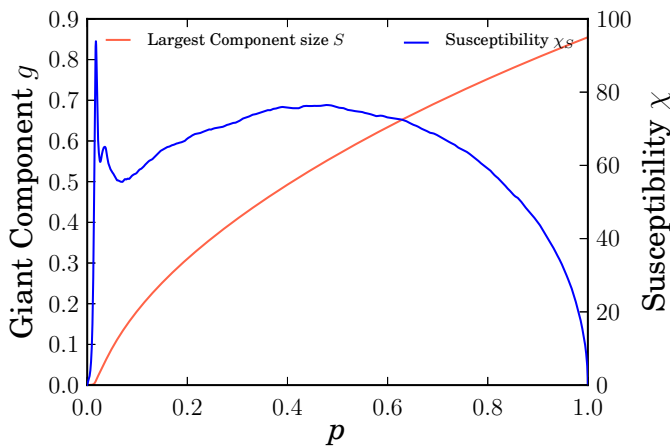


FIG. 13: Bond percolation simulations for the Epinions network. Left Size of the largest connected component  $S$  as a function of the bond occupation probability  $p$ . Right susceptibility  $\chi_S$  as a function of bond occupation probability  $p$ .

use of a pair of keys, one of them to encrypt the message, and its counterpart to decrypt the message. Both keys are generated in such a way that it is computationally infeasible to deduce one key from the other. Provided that everyone can generate a PGP key by himself, if anybody wants to know if a given key belongs really to the person stated in the key, he has to verify that. Hence exists a "signing procedure" where a person signs the public key of another, meaning that she trusts that the other person

is who she claims to be. This procedure generates a web of peers that have signed public keys of another based on trust, and this is the so-called web of trust of PGP [31]. Here, we analyze the web of trust as it was on July 2001, when it comprised 191.548 keys and 286.290 signatures. Since we are mainly interested in the social character of the web of trust we only consider bidirectional signatures, i.e., peers who have mutually signed their keys. This filtering process guarantees mutual knowledge between connected peers and makes the PGP network a reliable proxy of the underlying social network. After the filtering process, we are left with an undirected network of 57.243 vertices, 61.837 edges, average degree  $\bar{k} = 2.16$ , clustering coefficient  $\bar{C} = 0.50$  and maximum degree  $k_{max} = 205$ .

### 3. Epinions

This is a who-trust-whom online social network of a general consumer review site Epinions.com. Members of the site can decide whether to "trust" each other. All the trust relationships interact and form the Web of Trust which is then combined with review ratings to determine which reviews are shown to the user [32]. Here we consider the undirected network where users are connected if they "trust" each other. The resulting network has 31100 nodes, 103097 edges, an average degree of  $\bar{k} = 6.63$ , a clustering coefficient of  $\bar{C} = 0.24$  and a maximum degree of  $k_{max} = 443$ .

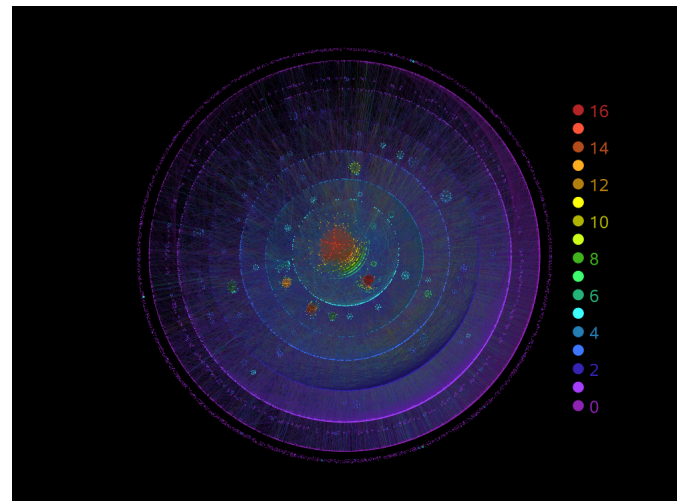


FIG. 14:  $m$ -core decomposition of the Epinions trust network.

- [1] R. Pastor-Satorras and A. Vespignani, Physical Review Letters **86**, 3200 (2001), ISSN 0031-9007.  
 [2] A. Lloyd and R. May, Science **292**, 1316 (2001), ISSN 0036-8075.  
 [3] M. Boguna, R. Pastor-Satorras, and A. Vespignani, Phys-

- ical Review Letters **90** (2003).  
 [4] G. Bianconi, Physics Letters A **303**, 166 (2002), ISSN 0375-9601.  
 [5] A. Goltsev, S. Dorogovtsev, and J. Mendes, Physical Review E **67** (2003), ISSN 1539-3755.

- [6] M. Hinczewski and A. N. Berker, *Physical Review E* **73** (2006), ISSN 1539-3755.
- [7] S. N. Dorogovtsev, A. V. Goltsev, and J. F. F. Mendes, *Reviews of Modern Physics* **80**, 1275 (2008), ISSN 0034-6861.
- [8] R. Cohen, K. Erez, D. Ben-Avraham, and S. Havlin, *Physical Review Letters* pp. 20–22 (2000).
- [9] D. S. Callaway, M. E. Newman, S. H. Strogatz, and D. J. Watts, *Physical Review Letters* **85**, 5468 (2000).
- [10] R. Cohen, D. Ben-Avraham, and S. Havlin, *Physical Review E* **66**, 036113 (2002), ISSN 1063-651X.
- [11] M. Newman, *Physical Review Letters* **89**, 208701 (2002), ISSN 0031-9007.
- [12] M. E. J. Newman and W.-w. Web, *Physical Review E* pp. 1–7 (2003), 0303183v1.
- [13] A. Vázquez and Y. Moreno, *Physical Review E* **67**, 015101 (2003), ISSN 1063-651X.
- [14] S. N. Dorogovtsev, J. F. F. Mendes, and A. N. Samukhin, *Phys. Rev. E* **64**, 066110 (2001).
- [15] V. L. Berezinskii, *Zh. Eksp. Teor. Fiz.* **59**, 907 (1970).
- [16] J. M. Kosterlitz and D. J. Thouless, *J. Phys. C* **6**, 1181 (1973).
- [17] S. V. Buldyrev, R. Parshani, G. Paul, H. E. Stanley, and S. Havlin, *Nature* **464**, 1025 (2010), ISSN 1476-4687.
- [18] S.-W. Son, G. Bizhani, C. Christensen, P. Grassberger, and M. Paczuski, *EPL* **97** (2012), ISSN 0295-5075.
- [19] G. J. Baxter, S. N. Dorogovtsev, A. V. Goltsev, and J. F. F. Mendes, *Physical Review Letters* **109** (2012), ISSN 0031-9007.
- [20] I. Kiss and D. Green, *Physical Review E* **78**, 048101 (2008), ISSN 1539-3755.
- [21] M. Newman, *Physical Review Letters* **103**, 058701 (2009), ISSN 0031-9007.
- [22] J. Miller, *Physical Review E* **80**, 020901 (2009), ISSN 1539-3755.
- [23] J. P. Gleeson, S. Melnik, and A. Hackett, *Physical Review E* **81**, 066114 (2010), ISSN 1539-3755.
- [24] M. Newman, *Physical Review E* **68**, 026121 (2003), ISSN 1063-651X.
- [25] J. Gleeson, *Physical Review E* **80**, 036107 (2009), ISSN 1539-3755.
- [26] M. Serrano and M. Boguñá, *Physical Review E* **74**, 056115 (2006), ISSN 1539-3755.
- [27] S. Melnik, A. Hackett, M. a. Porter, P. J. Mucha, and J. P. Gleeson, *Physical Review E* **83**, 036112 (2011), ISSN 1539-3755.
- [28] P. Colomer-de Simón, M. A. Serrano, M. G. Beiró, J. I. Alvarez-Hamelin, and M. Boguñá, *Scientific reports* **3**, 2517 (2013), ISSN 2045-2322.
- [29] M. E. Newman and R. M. Ziff, *Physical Review Letters* **85**, 4104 (2000), ISSN 0031-9007.
- [30] M. A. Serrano and M. Boguñá, *Phys. Rev. E* **74**, 056114 (2006).
- [31] M. Boguñá, R. Pastor-Satorras, A. Díaz-Guilera, and A. Arenas, *Physical Review E* **70**, 056122 (2004), ISSN 1539-3755.
- [32] M. Richardson, R. Agrawal, and P. Domingos, pp. 351–368 (2003).
- [33] Due to structural constraints, for very strong clustering it is not possible to keep  $\bar{c}(k)$  constant for very large values of  $k$ . In this case, the algorithm generates the maximum possible clustering [30]